International Journal of Engineering & Technology, 7 (3.29) (2018) 352-359

International Journal of Engineering & Technology

Website: www.sciencepubco.com/index.php/IJET

Research paper

Performance investigation of 3z buck boost converter for renewable applications

G. Kishor [1] *, M. Harsha Vardhan Reddy [2], K. Pushpalatha [2]

[1] Dept. of EEE, GPREC, Kurnool
[2] Associate Professor Dept. of EEE, GPREC, Kurnool
**Corresponding author E-mail: gudipatikishor@gmail.com*

Abstract

In case of renewable generation systems like Solar, Wind and Fuel cell it is required to use DC-DC converter to increase the voltage levels to meet demand. In such case the operating efficiency of dc-dc converter plays a vital role in energy conversion generally lie in the range of 60-80 percent. In this paper a 3-Z cascaded network is proposed for the renewable energy applications operating at higher efficiency. A comparison is made between conventional dc-dc buck boost converter with the proposed 3-Z cascaded network and analyzed its performance with lighting load. Simulation analysis is also performed to validate the proposed converter behavior.

Keywords: *About Four Key Words or Phrases in Alphabetical Order; Separated by Commas.*

1. Introduction

In recent years the application of DC-DC converter plays vital role in renewable generation systems like Solar power, Wind energy and other renewables. And it is required to have higher power quality and higher conversion efficiencies for this the use of power electronic converters is made mandate. Among all DC-DC converter configurations the Z-source converter is attaining major interest and has extraordinary components to meet higher voltage (both buck and boost) contrasted and the customary inverters [1]. It is x-modeled impedance or a lattice network arrangement called Z-source impedance network which couples the converter fundamental circuit to power source [14]. This network can be designed by the Fang Zheng Peng. The two traditional converters are voltage source inverters and current source inverter [20]. The Z-source converter utilizes an exceptional impedance system to couple converter fundamental circuit to power source, where a capacitor, inductor are used [6], separately. The Z-source converter (ZSC) uses passive components that can both buck, boost the input voltage. Converter main circuit is coupled to the power source by using passive components L and C to give the boosting of input voltage, which is not obtained in the conventional inverters [3]. By using the shoot through state which is present in Z source converter avoids the usage of the dead time which is used in conventional inverters to eliminate the risk of short circuit [8].

This network will perform better over the conventional converters such as VSI and CSI. The Z-source can be connected to all possible converter topologies. These converters and utilize an impedance organize, coupled between power source and converter circuit, to give both voltage buck operation and boost operation properties, which can't be accomplished with ordinary voltage source, current source converter. A two-port arrange that comprises of split-inductor, capacitors that are associated fit as a fiddle is utilized to give an impedance source (Z-source) coupling the inverter to dc source or battery.

The 3Z-network is shown in Fig 1 in which three dynamic Z-systems are joined. It is unique from the Z-source systems, which typically comprise of uninvolved components. In this 3Z-source converter, Z-arrangement 1 works as the main boost part, comprising of inductors L1, L2 and diodes D1, D2, and D3; Z-arrangement 2 is switch part, capacitor C1, and diodes D4 and D5; the second boost part is by Z-organize 3, comprises of L3, L4 and diodes D6, D7, and D8. A unique factor of the 3Z converter is only switched utilizing.

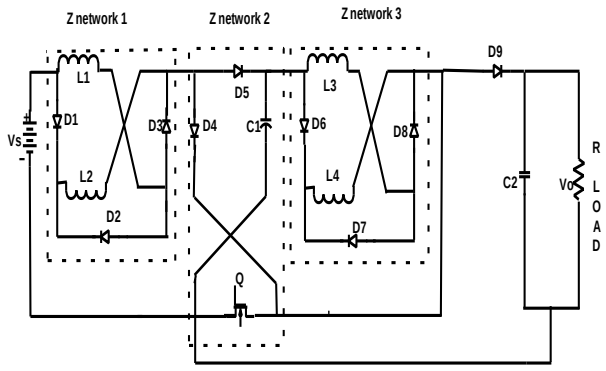

Fig. 1: 3 Z - Source Converter.

The 3Z-network converter can work both in CCM, DCM. Based on currents of the capacitors and diodes, six operational cases, includes two CCMs and four DCMs.

a) CCM mode

For straight forwardness, it is expected that

1) All the elements are ideal,
2) The free-wheeling diode of switch is disregarded,
3) L1 = L2 and L3 = L4.

In intermittent states (turn on, turn off) of switch Q, inductor stores and discharges energy, their currents increases and decreases. At that point, there relate a few cases to the present conditions of in-

ductors as current deceases and goes on to zero, is called the discontinuous current instance of inductors. Subsequently, the inductors can have constant or irregular current under some combinations of inductances, load, on period. The 3Z converter in CCM or DCM, at that point compare the six modes, i.e., six direct comparable circuits, separately explained.

In that, V_{L1}, V_{L2}, V_{L3}, and V_{L4} are voltages of L1, L2, L3, and L4 respectively, the clockwise as positive direction of reference currents, path shown in Fig 2 positive direction of the inductor reference voltages, the point by point conditions of the segments in circuits are shown in Table 1. Here, the 3Z converter execution in CCMs is explained in detail, i.e.,

Case 1: Mode 1 → Mode 2;

Case 2: Mode 1→ Mode 2→ Mode 3.

Table 1: Operating Modes

	Mode 1	Mode 2	Mode 3	Mode 4	Mode 5	Mode 6
Q	1	0	0	0	0	0
D1&D3	1	0	0	0	0	0
D2	0	1	1	1	0	0
D4	1	0	0	0	0	0
D5	0	1	1	1	0	0
D6&D8	1	0	0	0	0	0
D7	0	1	1	0	1	0
D9	0	1	1	0	1	0

Case 1:

In this case there are two types of operations based on pulses or depends on duty cycle. Those are Mode1 and Mode 2. As shown in Fig 2 and Fig 3 respectively. Modes 1 and Mode 2, circuits operation of switch Q, t_0 as the starts one period, t_1 as the mode progress moment from Mode 1 to Mode 2, and t_2 = T end of period. To describe the operation of converter in Case 1, key waveforms of 3Z converter in consistent state are shown in Fig 3, where two modes are shown in one period.

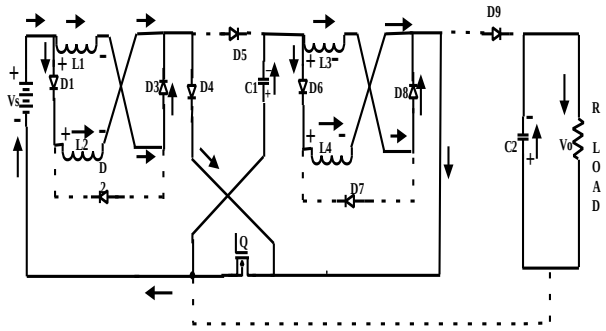

Fig. 2: Mode1 Operation.

1) Mode 1—t ∈ [t0, t1]: Q turns on, diodes D1, D3, and D4 are positive voltages and turn on simultaneously; then, D2 turns off due to negative voltage, L1, L2 are in parallel, after that reduce with D4, Q, and Vs to loop1. The source voltage Vs releases energy to L1 and L2, iL1, iL2 increases, and L1, L2 store energy, waveforms of iD1, iD3, iL1, and iL2 are shown in Fig 3(2), where iD1 = iD3 = iL1 = iL2, and iD4, is current of D4, continues iL1 + iL2, iD4 = iL1 + iL2 = 2iL1. These relations are given in equation (1)

$$iD1 = iD3 = iL1 = iL2$$

$$iD2 = 0 \quad (1)$$

$$i_{D4} = i_{D1} + i_{D3} = 2i_{L1}$$

$$V_{L1} = V_S$$

$$V_{L2} = V_S$$

Where V_{L1}, V_{L2} are the voltages of L1, L2, respectively.

In turn D5 and D7 have negative voltages and turn off, then D6 and D8 continue through positive voltages and turn on. L3 and L4 are parallel and after that reduce with Q and C1 to form loop 2. C1 releases energy to L3 and L4, and i_{L3} and i_{L4} increases. Hence, L3 and L4 stores energy. The waveforms of i_{D6}, i_{D8}, i_{L3}, and i_{L4} are shown in Fig 4(3), and waveform of i_{C1} is shown in Fig 4(4), where $i_{D6} = i_{D8} = i_{L3} = i_{L4}$, and $i_{C1} = -2i_{L3}$, respectively, and as given in equation (2).

$$i_{D6} = i_{D8} = i_{L3} = i_{L4}$$

$$i_{D5} = 0$$

$$iC1 = -2iL3 \quad (2)$$

$$VL3 = VC1$$

$$VL4 = VC1$$

Where i_{L3}, i_{L4}, V_{L3}, V_{L4}, and V_{C1} are the currents of L3, L4, and voltages of L3, L4, and C1, respectively. D9 has negative voltage and turns off, then capacitor C2 and load R are connected to form loop 3, C2 releases energy to R, output voltage of converter is V_o

$$VO = VC2 \quad (3)$$

Where V_C is voltage of capacitor C2.

2) Mode 2—t ∈ [t_1, t_2]: At t_1, Q turns off, mode changes from Mode 1 to Mode 2, as shown in Fig. 3, Q is off, D1, D3, D4, D6, and D8 goes negative voltage, turns off, then D2, D5, D7, and D9 turn on and then forms three loops in this mode. Loop 1 is V_S–L1–D2–L2–D5–C1, where V_s, L1, L2 release energy to C1, $V_s = V_{L1} + V_{L2} + V_C$, and i_{L1}, i_{L2} decreases as shown in Fig 4(2), currents of D2, D5 are equivalent to i_{L1}, and iC_1 increases as shown in Fig 4(4).

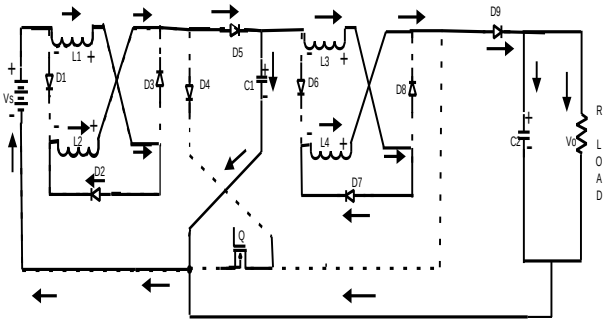

Fig. 3: Mode2 Operation.

$$i_{D2} = i_{D5} = i_{L1} = i_{L2}$$

$$i_{D1} = i_{D3} = i_{D4} = 0 \quad (4)$$

$$V_{L1} + V_{L2} = V_S - V_{C1}$$

Vs, L1, D2, L2, D5, L3, D7, L4, D9, and C2 forms loop, where Vs, L1, L2, L3, and L4 release the energy to C2 and R, $V_s = V_{L1} + V_{L2} + V_{L3} + V_{L4} + V_{C2}$, and i_{C2} decreases because of the release energy to the load R, i_{L3} and i_{L4} decreases as shown in Fig 4(3), and the currents of D7 and D9 are equivalent to i_{L3}.

$$i_{D7} = i_{D9} = i_{L3} = i_{L4}$$

$$i_{D6} = i_{D8} = 0 \quad (5)$$

$$V_{L3} + V_{L4} = V_S - (V_{L1} + V_{L2} + V_{C2}). \quad (6)$$

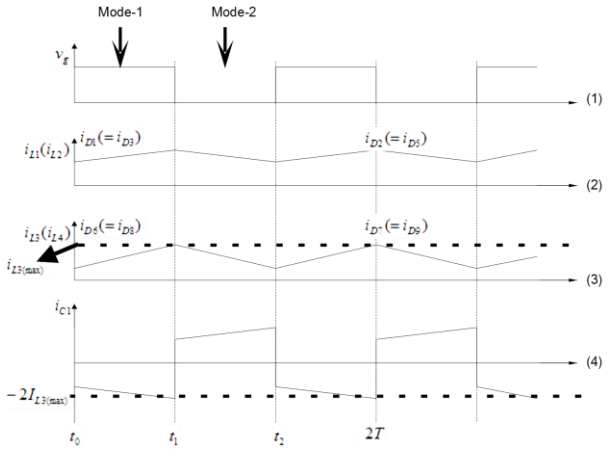

Fig. 4: Case1, Mode1 and Mode2 Key Waveforms of CCM.

Fig 4(1) shows determined voltage of switch Q; Fig 4(2) represents waveform of iL1 (iL2), two sections of waveform of iD1 = (iD3) and waveforms of iD2 = (iD5); Fig 4(3) waveform of iL3 (iL4), which is additionally made out of two sections of iD6 = (iD8) and the iD7 = (iD9); and Fig 4(4) shows waveforms of iC1. In that, iL1, iL2, iL3, iL4, iD1, iD2, iD3, iD5, iD6, iD7, iD8, iD9, iC1, and iC2 are the currents of L1, L2, L3, L4, D1, D2, D3, D5, D6, D7, D8, D9, C1, and C2, respectively.

b) Case 2:

In this case there are two types of operations based on their pulses or depends on the duty cycle. Those are Mode 1, Mode 2, and Mode 3. Cases 1 and 2 are both CCMs. There are three modes in Case 2 due to capacitor current iC_1, i.e., Modes 1, 2, and 3, whose identical circuits shown in Fig 2, Fig 3, Fig 4. Signify t_0 start of one period; t_1 as mode transition moment from Mode 1 to Mode 2, i.e., $t_1 = t_0 + DT$; t_2 as mode transition moment from Mode 2 to Mode 3, $t_3 = T$, at end of period. Operation procedure of converter, key waveforms of 3Z converter in Case 2 are shown in Fig 6.

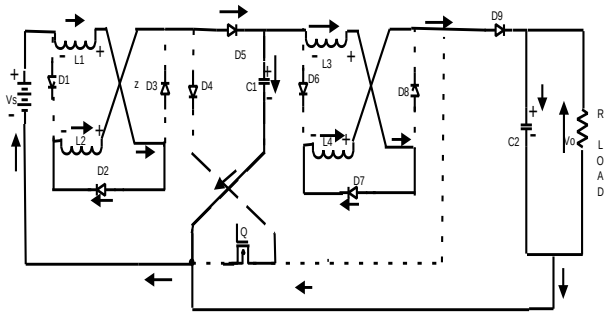

Fig. 5: Mode3 Operation.

Three modes are explained in one period. The operation procedure of the 3Z converter in a switch period is explained in the key waveforms as shown in Fig 6.

1) Mode 1—t ∈ [t_0, t_1]: The process is same as Mode 1 in Case 1. As shown in Fig 3.
2) Mode 2—t ∈ [t_1, t_2]: The process is same as Mode 2 in Case 1 apart from i_{C1}. i_{C1} reduces as shown in Fig 6(4), which is not same as increment of i_{C1} in Fig 4(4), that energy in inductors are insufficient to charge load.
3) Mode 3—t ∈ [t_2, t_3]: At t_2, i_{C1}, and i_{C2} reducing to 0, at that point Mode 3 starts, shown in Fig 5, waveforms are shown in Fig 6, where Q, D1, D3, D4, D6, D7, D8, and D9 are off, and D2, D5 are on, forms two loops.

Loop 1 is same as loop 1 in case 1. In loop 2, i_{C1} decreases from 0 to negative, which implies that V_s, L1, and L2 as well as C1 charge energy to circuit, and they satisfy conditions from Case 1.

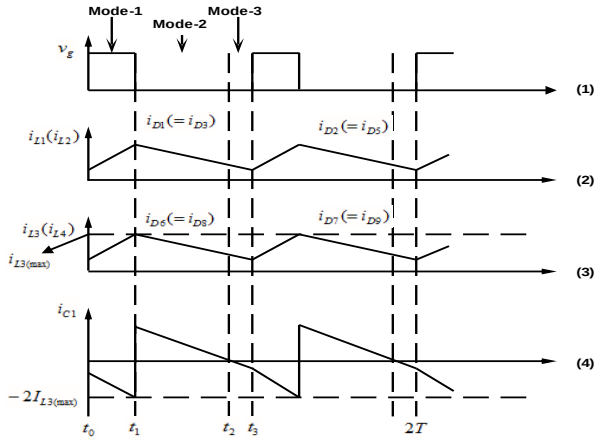

Fig. 6: Case2, Mode 1, Mode 2 and Mode 3 Key Waveforms in CCM Mode.

Here, the parameters of 3Z converter will be discussed and indicated by investigations above on operation of 3Z converter both in CCM. Parameters of converter are to be evaluated voltages and their currents of segments in circuit. The output voltage Vo will be considered as follows.

I. Output Voltage and Voltage Stress of Components:

As per discussion of Cases 1 and 2, output voltage V_o is derived as. As far as voltage second constant theory,

$$\int_0^{DT}(V_{L1}+V_{L2})dt+\int_{DT}^{T}(V_{L1}+V_{L2})dt=0 \tag{7}$$

Substituting (1)–(5) into (7) gives (8)

$$V_0=V_{C2}=V_s\left(\frac{1+D}{1-D}\right)^2$$

$$V_{C1}=V_s\left(\frac{1+D}{1-D}\right) \tag{8}$$

$$\int_0^{DT}(V_{L3}+V_{L4})dt+\int_{DT}^{T}(V_{L3}+V_{L4})dt=0 \tag{9}$$

$$\begin{aligned}&2V_sDT+(V_s-V_{C1})(1-D)T=0\\&2V_{C1}DT+(V_{C1}-V_0)(1-D)T=0\end{aligned} \tag{10}$$

From (8), the voltage of diodes is calculated above, output voltage Vop as,

$$V_{op}=\left((V_s-2V_D)\left(\frac{1+D}{1-D}\right)-2V_D\right)\left(\frac{1+D}{1-D}\right) \tag{11}$$

Where VD is voltage of the diodes. As per (9), connections of duty cycle D and voltage gain M = Vo/Vs in boost converters, 3Z converter can achieve a higher voltage gain than conventional boost converter, as (9) and (10), voltages of L1, L2, L3, and L4 can be as V_{L1}, V_{L2}, V_{L3}, and V_{L4} respectively, when Q is on and off, separately.

$$V_{L1}=V_{L2}=\left\{\begin{matrix}V_s,\\-V_s\left(\frac{D}{1-D}\right)\end{matrix}\right\} \tag{12}$$

If Q is on otherwise

$$V_{L3}=V_{L4}=\left\{\begin{matrix}V_s\left(\frac{1+D}{1-D}\right)\\-V_s\left(\frac{D(1+D)}{1-D}\right)\end{matrix}\right\} \tag{13}$$

2. Current components

By considering as lossless circuit then V_s. $I_{in} = V_o \cdot I_o$, where I_{in} and I_o are input, output currents, respectively, it gives the (14), Then I_{in} can be written as (14)

$$I_{in} = \frac{\int_0^{DT} 2i_{L1}dt + \int_{DT}^{T} i_{L1}dt}{T} = (1+D)I_{L1} \tag{14}$$

$$I_{in} = Io\left(\frac{(1+D)^2}{(1-D)^2}\right) \tag{15}$$

Substituting 4.15 into 4.14, then

$$i_{L1} = i_{L2} = I_o\left(\frac{(1+D)}{(1-D)^2}\right) \tag{16}$$

Thus, IL3 and IL4 can be given as

$$i_{L3} = i_{L4} = I_o\left(\frac{1}{1-D}\right) \tag{17}$$

As per (1), (2), (4), (5), and Fig 4 input currents of diodes are given as

$$I_{D2} = I_{D5} = (1-D)I_{L1} = I_o\left(\frac{(1+D)}{(1-D)}\right)$$

$$I_{D4} = 2DI_{L1} = I_o\left(\frac{2D(1+D)}{(1-D)^2}\right)$$

$$I_{D6} = I_{D8} = DI_{L3} = I_o\left(\frac{D}{(1-D)}\right) \tag{18}$$

a) Inductors Parameters:

The parameter of inductor is evaluated based on current and inductance, gives XL% (XL is pre assigned), output voltage Vo, output current Io, and for exchanging period T.

1) Determination of Rated Current: The evaluated currents of inductors are given from 4.16 and 4.17.
2) Determination of Rated Inductance: The ripples of inductors will have impact on the converter; therefore, inductance must be considered.

The inductors in converter have differential condition,

$$L = \frac{V_L dt_L}{di_L} \tag{19}$$

where VL is voltage of inductor as Q is on, dtL = DT is time of Q as it is on, and diL is inductor i.e., dtL.
Signify that IL by diL. diL is considered, XL% as

$$di_L = X_L\%i_L \tag{20}$$

Substituting (20) into (19) gives inductance of L, i.e

$$L = \frac{V_L dt_L}{X_L\%i_L} \tag{21}$$

Substituting voltage of inductors in (12), (13), in addition (16) and (17) into (21)

$$L1 = L2 = \frac{V_s DT}{X_L\%i_{L1}} = \frac{V_s D(1-D)^2 T}{X_L\%i_o(1+D)}$$

$$L3 = L4 == \frac{V_s(1+D)DT}{X_L\%i_{L3}(1-D)} = \frac{V_s(1+D)DT}{X_L\%i_o} \tag{22}$$

The inductance can be calculated $0 \le D \le 1$, for different values.

b) Parameters of Capacitors

The parameter of inductor, capacitor is to evaluated voltage and capacitance, given an allowed change, XC% (XC is pre assigned), output voltage Vo, output current Io, for exchanging period T.

1) Determination of Rated Voltage: The evaluated voltages of capacitors are solved as (9) and (10).
2) Determination of Rated Capacitance: The ripples of capacitors of converter, allowed can be varying to lan of capacitance. Then capacitors in converter is composed for differential condition of capacitors, i.e.,

Table 2: Load Regulation of the 3Z Converter

R Load (Ω)	Output voltage (V)	Input current (A)	Output current (A)	Input power (W)	Output power (w)	Efficiency (%)
175	23.2	0.28	0.13	3.36	3.016	89
200	23.2	0.25	0.11	3	2.552	85
220	23.2	0.23	0.1	2.76	2.32	84
240	23.2	0.21	0.09	2.52	2.088	82
260	23.2	0.2	0.089	2.4	2.064	84
280	23.2	0.19	0.082	2.28	1.856	83
300	23.2	0.17	0.077	2.04	1.786	80.2
320	23.2	0.165	0.072	1.98	1.624	8
340	23.2	0.15	0.068	1.92	1.577	82.1
360	23.2	0.53	0.064	1.83	1.48	81.1
380	23.2	0.146	0.061	1.75	1.415	8
400	23.2	0.14	0.058	1.68	1.345	8

3. Comparison between 3z converter and boost converter

Output power is calculated and tabulated for different load values of 3Z network boost converter as shown in Table 2. The output power is calculated and tabulated for the different load values of conventional boost converter as shown in Table 3. Fig 7 shows the graphical comparison of conventional boost and 3Z boost converter.

Table 3: Load Regulation of the Conventional Boost Converter

R Load (Ω)	Output voltage (V)	Input current (A)	Output current (A)	Input power (W)	Output power (w)	Efficiency (%)
175	116	6.6	0.66	79.2	76.56	96.6
200	116.4	6	0.58	72	67.28	93
220	116.4	6.1	0.52	73.2	60.32	82.4
240	116.4	5.4	0.48	64.8	55.68	85.9
260	116.4	5	0.45	60	52.2	87
280	116.4	4.7	0.42	56.4	48.72	86.3
300	116.4	4.6	0.389	55.4	45.124	81.7
320	116.4	4.5	0.365	54	42.34	78.4
340	116.4	4.1	0.334	49.2	38.74	78.7
360	116.4	4	0.32	48	37.12	77
380	116.4	4	0.306	48	35.49	73.9
400	116.4	3.8	0.29	45.6	33.64	73.7

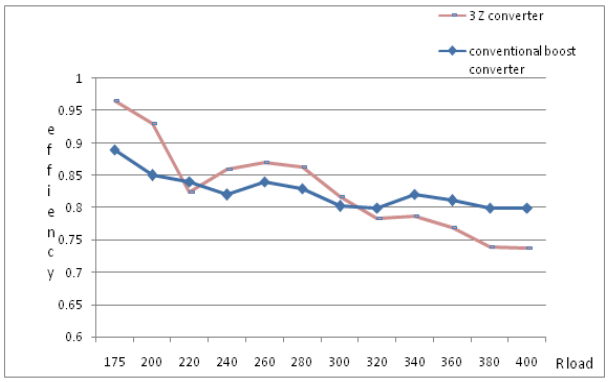

Fig. 7: Load vs Efficiency Graph for Conventional Boost Converter and 3Z Converter.

4. Simulation analysis

A 3Z Boost converter shown in Fig 1 is simulated with the design specifications of, power rating of 80W, 50% and 20% duty cycle, switching frequency

Fs =10 kHz, L1=L2=100µH, L3=L4=200µH, C1=220µF, C2=470µF and with a full load of RL=175Ω.

Fig 8 shows the supply voltage of 12V to the 3Z boost converter. The pulse pattern for the switch given in CCM is maintained at a duty ratio of 50% and as shown in Fig 9. And Fig 10 shows the input current of a 3Z converter during CCM, the input current attains a steady state average value of 9A at 0.15 sec. The input current ripple of the converter is as shown in Fig 11, the ripple current varies between 6A to 12A and maintains an average value of 9A. The frequency of one cycle of input current ripple is equal to the switching frequency.

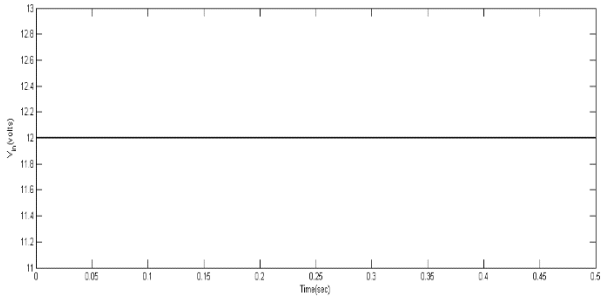

Fig. 8: Input Voltage of 3Z Converter in CCM.

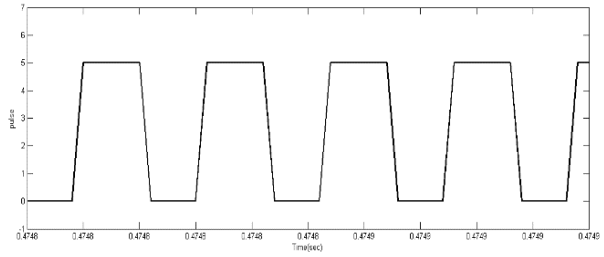

Fig. 9: Pulse Pattern of Switch Q of 3Z Converter in CCM.

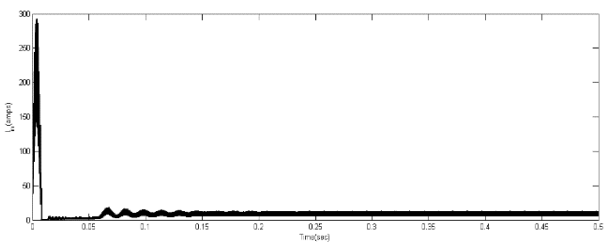

Fig. 10: Input Current of 3Z Converter in CCM.

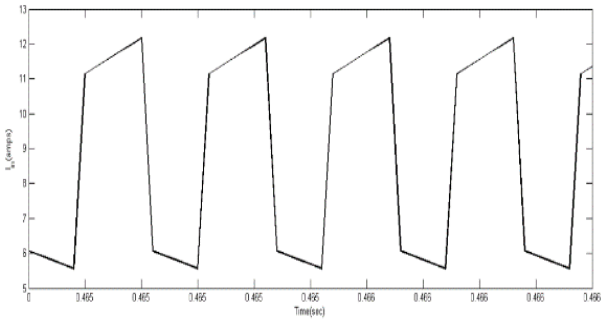

Fig. 11: Ripple in Input Current of 3Z Converter in CCM.

Fig 12 shows the current flowing through inductor L1 of a 3Z converter during CCM. The inductor current attains a steady state average value of 10A at 0.15 sec. The L1 inductor current ripple of the converter is as shown in Fig 13, the ripple current varies between 5.6A to 6.1A and maintains an average value of 5.8A. The frequency of one cycle of L1 inductor current ripple is equal to the switching frequency.

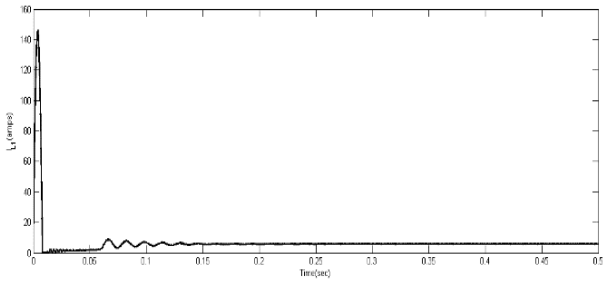

Fig. 12: Current through Inductor L1 of 3Z Converter in CCM.

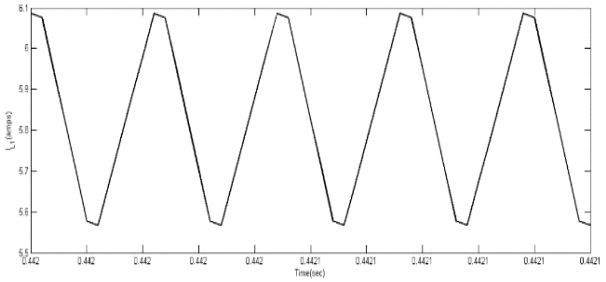

Fig. 13: Ripple in Inductor Current L1 of 3Z Converter in CCM.

Fig 14 shows the current flowing through inductor L3 of a 3Z converter during CCM. The inductor current attains a steady state average value of 3A at 0.15 sec. The L3 inductor current ripple of the converter is as shown in Fig 15, the ripple current varies between 1.2A to 2.2A and maintains an average value of 1.7A.
The frequency of one cycle of L3 inductor current ripple is equal to the switching frequency.

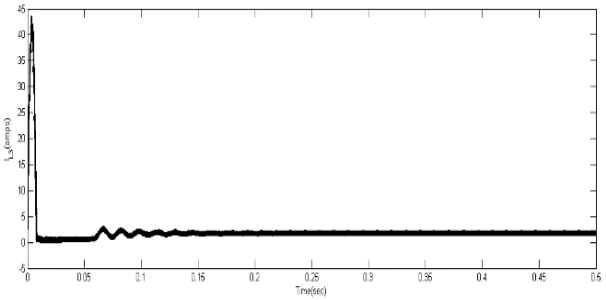

Fig. 14: Current through Inductor L3 of 3Z Converter in CCM.

Fig. 15 Ripple in inductor current L3 of 3Z converter in CCM
Fig 16 shows the current flowing through capacitor C1 of a 3Z converter during CCM. The capacitor current attains a steady state average value of 3A at 0.15 sec. The C1 capacitor current ripple of the

converter is as shown in Fig 17, the ripple current varies between -4.5A and maintains an average value of 0. The frequency of one cycle of C1 capacitor current ripple is equal to the switching frequency.

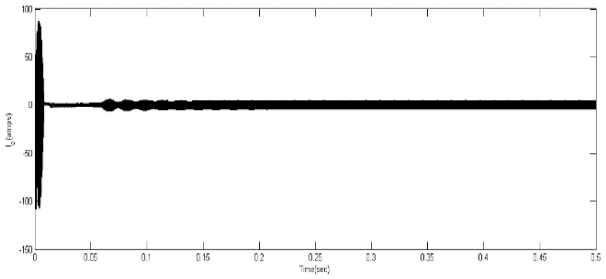

Fig. 16: Current through Capacitor C1of 3Z Converter in CCM.

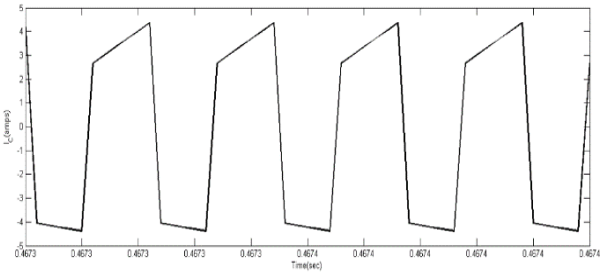

Fig. 17: Ripple in Capacitor Current C1 of 3Z Converter in CCM.

Fig 18 shows the output voltage of a 3Z converter during CCM and the output voltage attains a steady state average value of 116V at 0.15 sec. The output voltage ripple of the converter is as shown in Fig 19, the ripple voltage varies between 116.36V to 116.37V and maintains an average value of 116.366V. The frequency of one cycle of input current ripple is equal to the switching frequency.

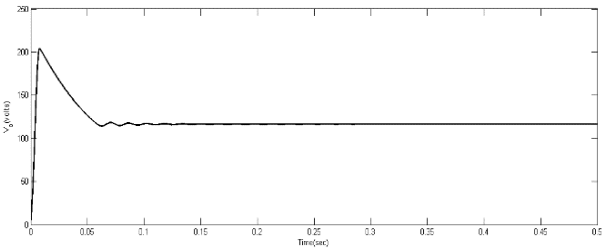

Fig. 18: Output Voltage of 3Z Converter in CCM.

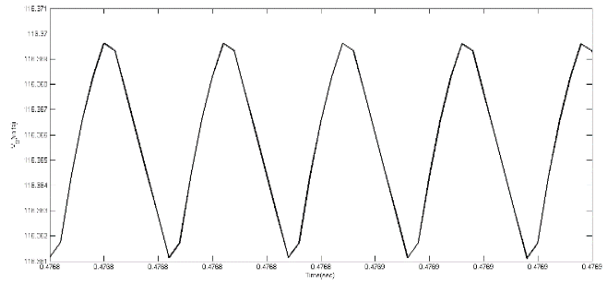

Fig. 19: Ripple in Output Voltage of 3Z Converter in CCM.

The performance of the 3Z-source boost converter is verified in the CCM mode by using Matlab/Simulink. The results of the 3Z-source converter are shown from Fig 8-19. It is observed that the frequency of each cycle is equal to switching frequency. At full load, the efficiency of the converter is 96%, and for the different loads the converter is simulated and the efficiency of the converter at different loads are tabulated, as shown in the Table 3.

5. Closed loop control of 3z network dc-dc converter

To simplify the use of consistent time, detailed analysis on P-I-D controllers is required. In initial state of the repetition, it was expected to exhibit how the P, P-I, P-I-D controllers. In addition, methods to tune P-I-D controllers were presented. It is intended to demonstrate s how hard it could get to appropriately tune a P-I-D controller. Furthermore, it is projected to indicate how P, P-D, P-I, and P-I-D controllers influence the transient reaction of the shut loop framework. Demonstrate how to boost up a component can however lose the other. Thirdly, it was expected to indicate how one should assess flow of ceaseless time plant and utilize legitimate testing time for discrete time P-I-D controller.

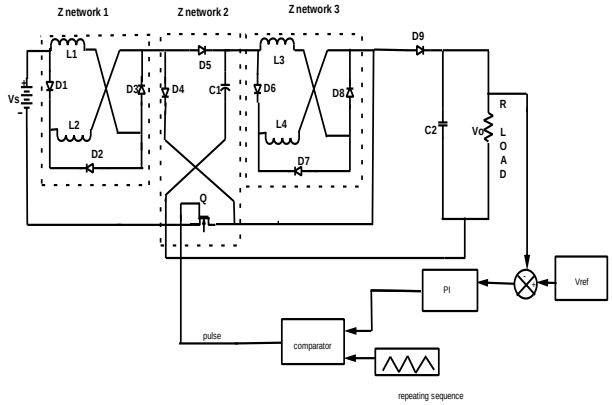

Fig. 20: PI Controller of 3Z Network.

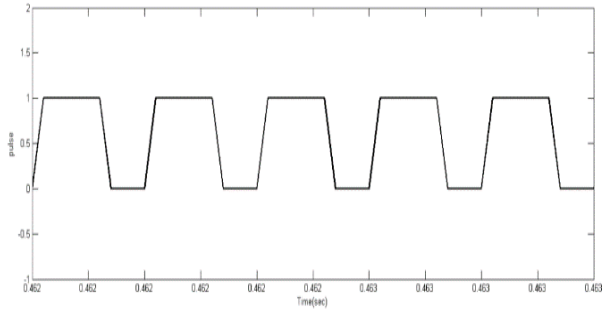

Fig. 21: Pulse Pattern of Switch Q of 3Z Converter Using PI Controller.

The schematic diagram of a 3Z converter in closed loop control is shown in Fig 20, since PI controller is having more advanced when compare to other controller PI controller is used in controlling the converter. The parameters used in section II are used for simulating the converter in closed loop. The constants of the PI controller, Kp=0.06 and Ki=10 are considered based on the trial and error processes. This value of converter with a supply voltage of 12V and steady state output of converter is 320V at 0.15 sec.

Fig 22 shows the output voltage of a 3Z converter using PI controller, it reaches a finite value at 320V at 0.15 sec. The harmonic spectra ripple waveform is shown Fig 23, the ripple voltage varies between 316 to 326V and maintains mean of 320V. The frequency of one cycle of input current ripple is equal to the switching frequency.

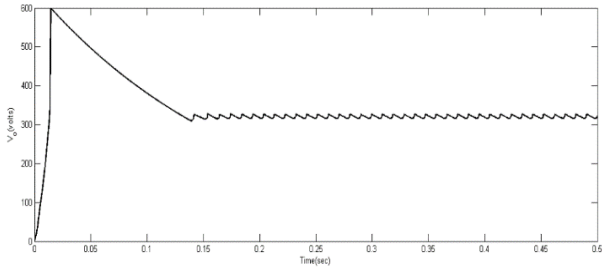

Fig. 22: Output Voltage of 3Z Converter Using PI Controller.

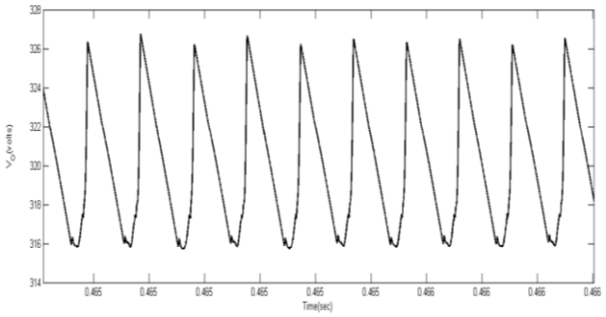

Fig. 23: Ripple in Output Voltage of 3Z Converter Using PI Controller.

The schematic diagram of a 3Z converter in closed loop control using fuzzy is shown in Fig 24, since artificial intelligence technique is having more advantages when compared to the analog technique controller, therefore a 3Z network with fuzzy controller is used. The parameters used in section II are used for simulating the converter in closed loop. The value of converter with a supply voltage of 12V and steady state output of converter is 320V at 0.13 sec.

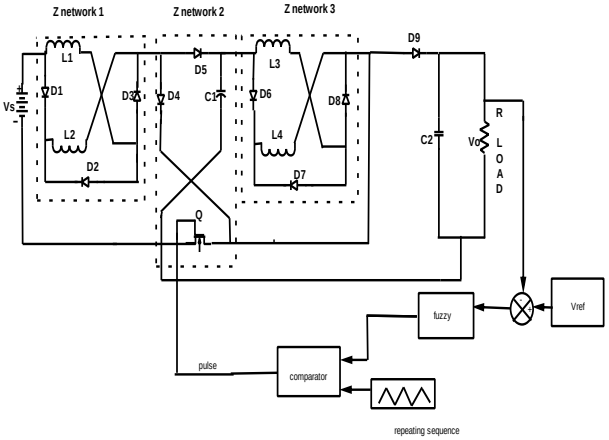

Fig. 24: Fuzzy Controller of 3Z Network.

Fig. 25 shows the waveform for voltage across the load for 3Z converter using fuzzy controller, it reaches finite value of 320V at 0.13 sec. The harmonic content of the waveform is represented in Fig 26; it ranges in between the values of 315.303 to 315.316V settles to 315.303V.

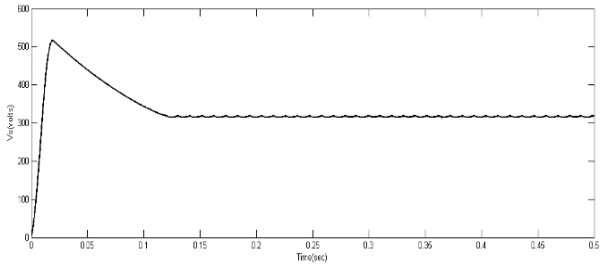

Fig. 25: Output Voltage of 3Z Converter with Fuzzy Controller.

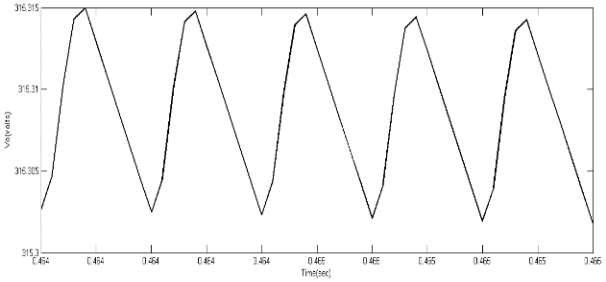

Fig.26: 16 Ripple in Output Voltage of 3Z Converter with Fuzzy Controller.

6. Conclusion

The 3Z network DC-DC converter for boost operation, it includes three z networks interconnected in series, in which only one switch is utilized. It provides a high voltage gain where required for most industrial applications. The 3Z converter is analyzed in continuous current mode (CCM). Detailed design aspects were studied and implemented for the effectiveness of the 3Z-network DC-DC Converter. A feedback system is implemented for the converter with proportional and integral controllers for steady state analysis. With the advantages in intelligent control techniques a rule based system is introduced to improve the performance of the converter under distinct modes of operations. The 3Z network converter with closed loop control systems is modeled using MATLAB/Simulink. The simulations obtained validate the improved performance of the converter circuit.

References

[1] W. Li, J. Liu, J. Wu, and X. He, "Design and analysis of isolated ZVT boost converters for high-efficiency and high-step-up applications," IEEE Trans. Power Electron., vol. 22, no. 6, pp. 2263–2374, Nov. 2007.

[2] E. H. Ismail, M. A. Al-Saffar, A. J. Sabzali, and A. A. Fardoun, "A family of single-switch PWM converters with high step-up conversion ratio," IEEE Trans. Circuits Syst. I, Reg. Papers, vol. 55, no. 4, pp. 1159–1171, May 2008.

[3] M. A. Al-Saffar, E. H. Ismail, and A. J. Sabzali, "Family of ZC-ZVS converters with wide voltage range for renewable energy systems," Renew. Energy, vol. 56, pp. 32–43, Aug. 2013.

[4] W. Y. Choi and C. G. Lee, "Photovoltaic panel integrated power conditioning system using a high efficiency step-up DC–DC converter," Renew. Energy, vol. 41, pp. 227–234, May 2012.

[5] J.-C. Tsai, Modified Hysteretic Current Control (MHCC) for improving transient response of boost converter," IEEE Trans. Circuits Syst. I, Reg. Papers, vol. 58, no. 8, pp. 1967–1979, Aug. 2011.

[6] X. G. Feng, J. J. Liu, and F. C. Lee, "Impedance specifications for stable DC distributed power systems," IEEE Trans. Power Electron., vol. 17, no. 2, pp. 157–162, Mar. 2002.

[7] Y. Tang, T. Wang, and Y.He, "A switched-capacitor-based active-network converter with high voltage gain," IEEE Trans. Power Electron., vol. 29, no. 6, pp. 2959–2968, Jun. 2014.

[8] K. I. Hwu, C. F. Chuang, andW. C. Tu, "High voltage-boosting converters based on bootstrap capacitors and boost inductors," IEEE Trans. Ind. Electron., vol. 60, no. 6, pp. 2178–2193, Jun. 2013.

[9] C.-M. Young, M.-H.Chen, T.-A. Chang,C.-C. Ko, and K.-K. Jen, "Cascade Cockcroft–Walton voltage multiplier applied to transformerless high step-up DC–CDC converter," IEEE Trans. Ind. Electron., vol. 60, no. 2, pp. 523–537, Feb. 2013.

[10] D. S. Wijeratne and G. Moschopoulos, "Quadratic power conversion for power electronics: Principles and circuits," IEEE Trans. Circuits Syst. I, Reg. Papers, vol. 59, no. 2, pp. 1967–1979, Feb. 2011.

[11] G. A. L. Henn, R. N. A. L. Silva, P. P. Praca, L. H. S. C. Barreto, and D. S. Oliveira, Jr., "Interleaved-boost converter with high voltage gain,"IEEE Trans. Power Electron., vol. 25, no. 11, pp. 2753–2761, Nov. 2010.

[12] W. C. Li, X. Xiang, C. S. Li, W. H. Li, and X. He, "Interleaved high step-up ZVT converter with built-in transformer voltage doubler cell for distributed PV generation system," IEEE Trans. Power Electron., vol. 28, no. 1, pp. 300–313, Jan. 2013.

[13] D. Li, P. C. Loh, M. Zhu, G. Feng, and F. Blaabjerg, "Generalized multicell switched-inductor and switched-capacitor Z-source inverters," IEEE Trans. Power Electron., vol. 28, no. 2, pp. 837–848, Feb. 2013.

[14] W. Qian, F. Z. Peng, and H. Cha, "Trans-Z-source inverters," IEEE Trans. Power Electron., vol. 26, no. 12, pp. 3453–3463, Feb. 2011.

[15] M. S. Shen et al., "Constant boost control of the Z-source inverter to minimize current ripple and voltage stress," IEEE Trans. Ind. Appl., vol. 42, no. 3, pp. 770–778, May/Jun. 2006.

[16] Y. Li, S. Jiang, J. G. Cintron-Rivera, and F. Z. Peng, "Modeling and control of quasi-Z-source inverter for distributed generation applications," IEEE Trans. Ind. Electron., vol. 60, no. 4, pp. 1532–1541, Apr. 2013.

[17] V. P. Galigekere N and M. K. Kazimierczuk, "Analysis of PWM Z-source DC-DC converter in CCM for steady state," IEEE Trans. Circuits System. I, Reg. Papers, vol. 59, no. 4, pp. 854–863, Apr. 2012.

[18] G. N. Veda Prakash and M. K. Kazimierczuk, "Small-signal modeling of open-loop PWM Z-source converter by circuit-averaging technique," IEEE Trans. Power Electron., vol. 28, no. 3, pp. 1286–1296, Mar. 2013.
[19] D. Vinnikov and I. Roasto, "Quasi-Z-source-based isolated DC/DC converters for distributed power generation," IEEE Trans. Ind. Electron., vol. 58, no. 1, pp. 192–201, Jan. 2011.
[20] F. Z. Peng, "Z-source inverter," IEEE Trans. Ind. Appl., vol. 39, no. 2, pp. 504–510, Mar. 2003.
[21] W. Li et al., "Series asymmetrical half-bridge converters with voltage autobalance for high input-voltage applications," IEEE Trans. Power Electron., vol. 28, no. 8, pp. 3665–3674, Aug. 2013.
[22] J. C. Rosas-Caro, F. Z. Peng, H. Cha, and C. Rogers, "Z-source-converterbased energy-recycling zero-voltage electronic loads," IEEE Trans. Ind. Electron., vol. 56, no. 12, pp. 4894–4902, Dec. 2009.
[23] C. Mario, C. Alfio, A. Rosario, and G. Francesco, "Soft-switching converter with HF transformer for grid-connected photovoltaic systems," IEEE Trans. Ind. Electron., vol. 57, no. 5, pp. 1678–1686, May 2010.
[24] B. M. Ge, Q. Lei, W. Qian, and F. Z. Peng, "A family of Z-source matrix converters," IEEE Trans. Ind. Electron., vol. 59, no. 1, pp. 35–46, Jan. 2012.